

## CFD MODELLING OF NEW DESIGNED HEAT EXCHANGER

Viktor Trokhaniak<sup>1</sup>, Dainis Viesturs<sup>2</sup>, Adolfs Rucins<sup>2</sup>, Yevhenii Bakulin<sup>1</sup>,  
Oleksandr Synyavskiy<sup>1</sup>, Larysa Kolomyets<sup>3</sup>, Valentina Bakulina<sup>1</sup>

<sup>1</sup>National University of Life and Environmental Sciences of Ukraine, Ukraine;

<sup>2</sup>Latvia University of Life Sciences and Technologies, Latvia;

<sup>3</sup>National Scientific Center "Institute of Agriculture"  
of the National Academy of Agrarian Sciences of Ukraine, Ukraine  
adolfs.rucins@lbtu.lv

**Abstract.** This paper investigates the thermohydrodynamic processes in a newly designed shell-and-tube heat exchanger with a compact tube bundle arrangement under conditions of cross-flow air circulation. The need for this study arises from the fact that increasing the heat transfer intensity in compact heat exchangers is often accompanied by an increase in hydraulic resistance, uneven distribution of heat transfer fluids, and incomplete utilisation of the heat transfer surface. Therefore, for further design improvements, it is necessary to determine not only the integral thermal performance parameters but also the local fields of velocity, temperature, pressure and heat flux in the inter-tube space and the tube channel. Numerical modelling was performed in ANSYS Fluent based on the Navier–Stokes equations and the energy equation, using the RNG k- $\epsilon$  turbulence model. A heat exchanger with a rectangular cross-section, a compact single-row arrangement of smooth tubes, an air flow rate of  $0.1389 \text{ kg}\cdot\text{s}^{-1}$  at a temperature of  $+40 \text{ }^\circ\text{C}$  and a water flow rate of  $0.2778 \text{ kg}\cdot\text{s}^{-1}$  at a temperature of  $+5 \text{ }^\circ\text{C}$  was considered. It has been established that local air acceleration in the inter-tube channels up to  $20\text{--}30 \text{ m}\cdot\text{s}^{-1}$  ensures a reduction in its temperature from  $40$  to  $28.64 \text{ }^\circ\text{C}$  and the formation of a heat flux on the wall of up to  $1500\text{--}1568 \text{ W}\cdot\text{m}^{-2}$ . The water temperature in this case increases from  $5$  to  $37.75 \text{ }^\circ\text{C}$  at a velocity of  $0.245\text{--}0.248 \text{ m}\cdot\text{s}^{-1}$ . It has been shown that the intensification of heat transfer is accompanied by an increase in pressure losses of up to  $780 \text{ Pa}$  for air and  $1200 \text{ Pa}$  for water. Non-uniformity in velocity and temperature fields has been identified, caused by recirculation zones in the manifolds, flow separation along the pipes, and non-uniform air distribution between the central and wall channels. The results obtained justify the need for the next stage of research, aimed at optimising the geometry of the inter-tube space, reducing recirculation zones, smoothing the air flow, and reducing hydraulic losses whilst maintaining high heat transfer intensity.

**Keywords:** heat exchanger, CFD modelling, compact tube bundle, heat and mass transfer, hydraulic losses.

### Introduction

Heat exchangers are vital components of energy and process systems, designed to transfer thermal energy between heat transfer fluids at different temperature levels. Their use enables improved thermal control efficiency and reduced energy losses in engineering systems [1]. One of the most common types of heat exchange equipment is shell-and-tube heat exchangers, which are widely used in air conditioning systems, the power industry, the chemical industry and the aerospace sector [2]. Depending on the design of the tube bundle, a distinction is made between straight-tube heat exchangers and heat exchangers with U-shaped tubes, in which the coolant flow changes direction in the bend of the tubes.

Improving the efficiency of shell-and-tube heat exchangers is the subject of numerous studies. Experimental methods allow for reliable results but require significant material costs. Consequently, numerical modelling methods have become widely used, as they enable the investigation of thermohydrodynamic processes in complex geometric structures. The ANSYS Fluent software package is frequently employed for such studies, as it allows the analysis of velocity, temperature and pressure fields at any point within the heat exchanger [3].

One of the main approaches to increasing heat transfer intensity is to increase the turbulence of the coolant flow. Methods for intensifying heat transfer are conventionally divided into active and passive methods [4]. Active methods involve the use of external energy sources, in particular mechanical or electrohydrodynamic effects on the flow [5]. Passive methods are based on modifying the geometry of the channels or the heat transfer surface. The most common passive methods include the use of expanded heat transfer surfaces (fins), twisted tubes, spiral strips and vortex generators, which help increase turbulence and enhance heat transfer intensity [6-8].

A separate area of research is optimisation of the heat exchanger design. For instance, M.A. Jamil et al. [9] applied exergetic optimisation, which enabled a reduction in the heat exchange area by approximately 26.4%, capital costs by 20%, and operating costs by almost 50%. In the work by Lim & Choi [10], the use of the cooling energy of liquefied natural gas for cooling the jacket of an internal

combustion engine was investigated, where it was established that the working fluid R123 provides a thermal efficiency of 17-23% and the highest exergetic efficiency (25-31%).

An important factor in improving the efficiency of heat transfer processes is the optimisation of the tube bundle geometry. According to the results of studies [11], the transverse displacement of adjacent tubes relative to the flow helps improve the overall heat transfer characteristics, although it simultaneously leads to an increase in pressure losses. For pipes with a diameter of 10 mm, the optimal offset is approximately 1-3 mm. Further studies have shown that such intensification of heat exchange does not require a significant increase in the power of the pumping equipment used to circulate the coolant in the inter-tube space of the heat exchanger [12].

An analysis of current approaches to the development and improvement of heat exchangers highlights the relevance of research aimed at optimising the design of shell-and-tube heat exchangers. In particular, the development of new and the improvement of existing designs of heat exchangers with compact tube bundle arrangements, which allows for increased heat transfer intensity and improved mass-dimensional characteristics of the equipment, is of considerable scientific interest.

The aim of the study is to improve existing and develop new design solutions for shell-and-tube heat exchangers featuring a compact arrangement of smooth-tube bundles with cross-flow, as well as to perform numerical modelling of heat and mass transfer processes in the channels of such heat exchangers.

### Materials and methods

A shell-and-tube heat exchanger (HE) is considered, designed as a compact configuration with a rectangular cross-section and cross-flow (Fig. 1). The heat exchanger utilises a system of tubes arranged in a single row, in which adjacent tubes are in contact with one another. This is due to the fact that modern, relatively inexpensive technologies for manufacturing such bundles are significantly complicated when the distance between the tubes is less than 5 mm. The HE consists of three manifolds, each containing 5 rows and 10 tubes in depth. The passage width in TA is 80 mm, with a length of 356 mm. The tubes touch one another along the air flow, creating a channel that differs from a corridor arrangement. The mass flow rate of air at the heat exchanger inlet was taken to be  $500 \text{ kg}\cdot\text{h}^{-1}$ , which, when converted to SI units, and corresponds to  $0.1389 \text{ kg}\cdot\text{s}^{-1}$ . The initial air temperature was  $+40 \text{ }^\circ\text{C}$  (mass-flow inlet). At the air outlet, a zero-gauge pressure condition was applied (pressure outlet). The mass flow rate of water was taken as  $1000 \text{ kg}\cdot\text{h}^{-1}$ , which corresponds to  $0.2778 \text{ kg}\cdot\text{s}^{-1}$ , at an initial temperature of  $+5 \text{ }^\circ\text{C}$  (mass-flow inlet). At the water outlet, a zero-gauge pressure condition was also applied (pressure outlet). The external walls of the casing were treated as stationary no-slip walls without heat loss to the environment (adiabatic wall). Heat transfer between the air, the tube wall and water was modelled using coupled thermal wall conditions (coupled wall). This flow rate ratio was adopted as the design operating mode of the heat exchanger for assessing the heat transfer intensity and hydraulic losses in the compact tube bundle. The height of the tubes is 200 mm, with an outer diameter of 10 mm and a wall thickness of 1 mm. The metal material is Steel-3. The heat exchanger was originally designed to reduce the air temperature to  $+25 \text{ }^\circ\text{C}$ . The flow of heat transfer fluids in the heat exchanger is counter-current.

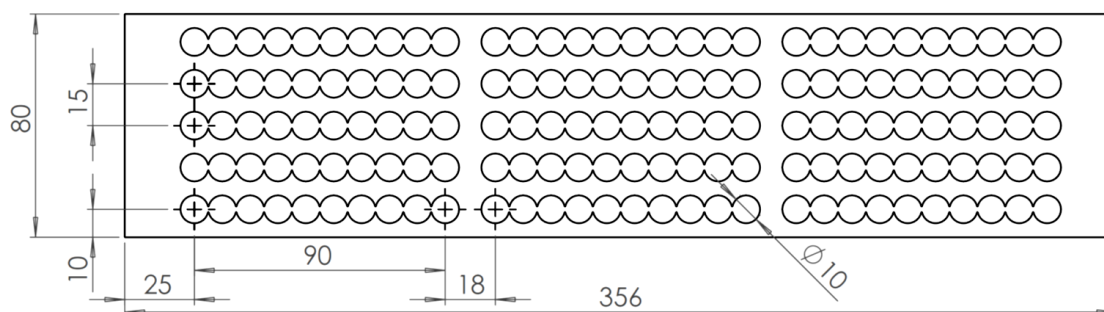


Fig. 1. Tube board with a compact tube layout (top view)

Numerical modelling of heat and mass transfer processes in the channels of compact-configuration heat exchangers was carried out using ANSYS Fluent software. The mathematical model is based on

the Navier–Stokes equations and the convective energy transfer equation. The RNG  $k$ - $\varepsilon$  turbulence model was selected.

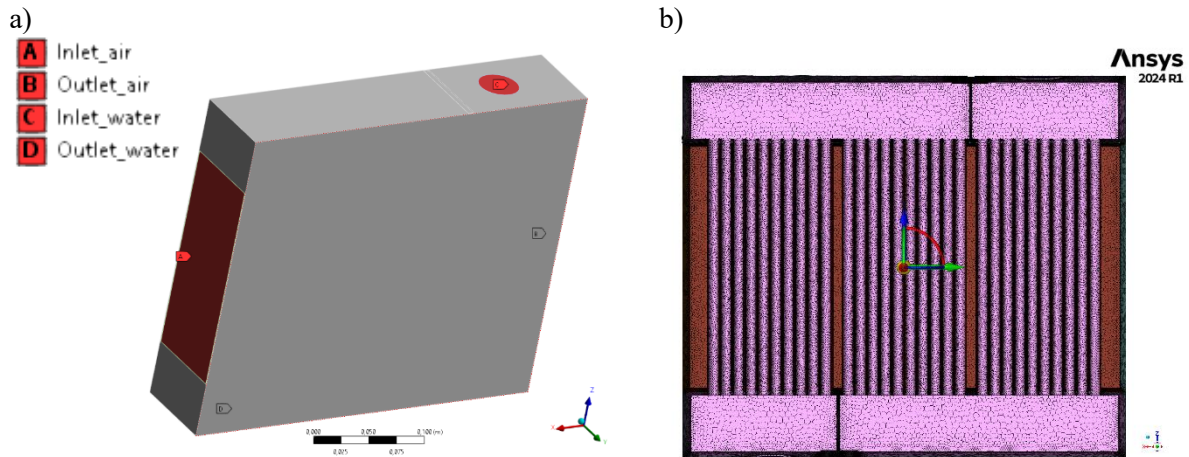


Fig. 2. Heat exchanger: a – boundary conditions, b – mesh

Fig. 2 shows the computational domain with boundary conditions (Fig. 2a) and the mesh (Fig. 2b). The mesh was constructed using the poly-hexcore volume element method. As a result, we obtained: nodes: 107,355,451; edges: 336,559; faces: 158,226,350; cells: 31,333,163. The minimum face size is 0.4 mm, and the maximum is 6.4 mm. The mesh quality according to the Orthogonal quality criterion is 0.208. When generating the mesh in ANSYS Fluent Meshing and performing the direct simulation in ANSYS Fluent, 221 GB of RAM was utilised out of the 256 GB available.

## Results and discussion

Figs 3-5 show the distributions of temperature, velocity and pressure in the heat exchanger channels for air and water.

For the liquid coolant (water) flowing through the tube space, the average velocity at the inlet is  $0.245 \text{ m}\cdot\text{s}^{-1}$ , and at the outlet –  $0.248 \text{ m}\cdot\text{s}^{-1}$ . Thus, the change in velocity does not exceed 1.3%, indicating a steady flow regime without significant redistribution of flow rate across the tubes. In most of the channel, the velocity is within the range of  $0.20$ - $0.30 \text{ m}\cdot\text{s}^{-1}$  (Fig. 3a). At the same time, local velocity values in the inlet and outlet sections can reach  $0.45$ - $0.50 \text{ m}\cdot\text{s}^{-1}$ , which is due to the geometry of the collectors.

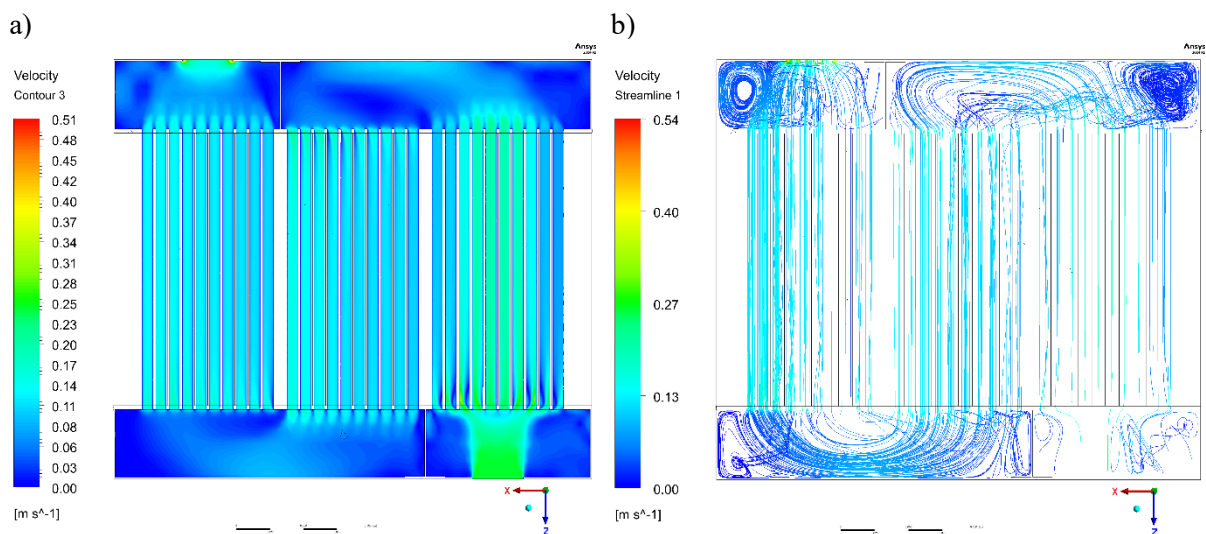


Fig. 3. Velocity field (a) and streamlines (b) along the  $zx$  centreline in the water-coolant channel of a compact tube bundle,  $\text{m}\cdot\text{s}^{-1}$

Analysis of the flow lines (Fig. 3a) shows that the inlet and outlet chambers are characterised by the presence of recirculation zones. In these regions, the flow velocity drops to values below  $0.05$ -

$0.10 \text{ m}\cdot\text{s}^{-1}$ . Such zones occupy up to 15-20% of the chamber volume and lead to uneven distribution of the coolant throughout the tube bundle.

For the gaseous coolant (air) flowing in the intertube space, the average velocity varies from  $7.70 \text{ m}\cdot\text{s}^{-1}$  at the inlet to  $8.11 \text{ m}\cdot\text{s}^{-1}$  at the outlet, corresponding to an increase of approximately 5.4%. At the same time, the flow pattern is significantly more non-uniform. The main part of the flow moves at speeds ranging from  $10\text{-}18 \text{ m}\cdot\text{s}^{-1}$  (Fig. 4a), whilst in the inter-tube channels local acceleration of the flow up to  $20\text{-}28 \text{ m}\cdot\text{s}^{-1}$  is observed. At certain points, the velocity can reach  $30\text{-}32 \text{ m}\cdot\text{s}^{-1}$ .

Analysis of the obtained distributions shows that the velocity in the inter-tube channels is 2-3 times higher than the average flow velocity. This is due to the narrowing of the flow cross-section and the formation of a jet-like flow structure (Fig. 4b). At the same time, regions of reduced velocities (less than  $5 \text{ m}\cdot\text{s}^{-1}$ ) form behind the pipes, corresponding to areas of flow separation and the formation of vortex structures.

It is characteristic that near the casing walls, the flow velocity is 1.5-2 times higher than the velocity in the central channels. This leads to redistribution of the coolant flow and reduction in the efficiency of the outer rows of tubes.

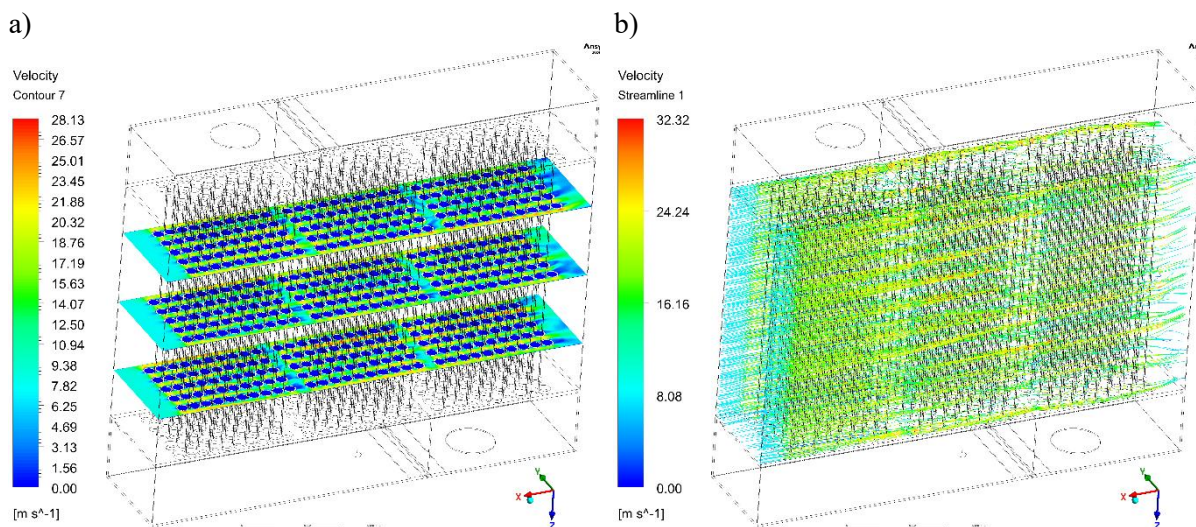


Fig. 4. Velocity field (a) and streamlines (b) in the 3D air flow around a compact tube bundle,  $\text{m}\cdot\text{s}^{-1}$

The results obtained show that the intensification of heat transfer in the structure under investigation is achieved through local acceleration of the flow in the inter-tube channels. However, the presence of recirculation zones within the chambers and behind the tubes may lead to additional hydraulic losses and non-uniform heat transfer along the length of the bundle. Analysis of the results obtained shows that the flow behaviour of the heat transfer fluids differs significantly.

The measured velocity values allow the flow regime of the coolants to be assessed. For air, at an average velocity of  $7.7\text{-}8.1 \text{ m}\cdot\text{s}^{-1}$  and a characteristic channel size of approximately 5 mm, the Reynolds number is approximately  $Re \approx 2000\text{-}3000$ , and in local acceleration zones ( $24 \text{ m}\cdot\text{s}^{-1}$ ) it can reach  $Re \approx 15000$ . This corresponds to transitional and turbulent flow regimes, which ensures intensified heat transfer in the inter-tube channels. For water at a velocity of  $0.11\text{-}0.25 \text{ m}\cdot\text{s}^{-1}$ , the Reynolds number does not exceed  $Re \approx 2000\text{-}3000$ , which corresponds to laminar or transitional flow. Thus, the main contribution to heat transfer comes from the gaseous heat carrier. Given that a local increase in velocity by a factor of 2-3 leads to an increase in the Nusselt number by approximately 1.5-2 times, it can be concluded that the geometry of the compact tube bundle ensures an increase in heat transfer intensity without a significant increase in the average coolant flow rate. At the same time, the presence of zones with reduced velocities limits the realisation of the heat transfer potential and indicates the need for further optimisation of the channel geometry, particularly in the region of the inlet chambers and the near-surface zones of the casing. Reducing the distance from the casing to the outermost row of tubes from 5 mm to 2 mm will redistribute the air flow more towards the other channels, which in turn will increase the heat transfer intensity.

The Figs shown illustrate the temperature distribution within the heat exchanger channels, enabling an assessment of the intensity and nature of heat transfer between the heat transfer fluids. According to the results of numerical modelling, the inlet air temperature is 40 °C, whilst at the outlet it drops to 28.64 °C, corresponding to a decrease of 11.36 °C (Fig. 5a). At the same time, the water temperature varies from 5.0 °C to 37.75 °C, i.e. the increase is 32.75 °C (Fig. 5b). This difference indicates a significant intensity of heat exchange and effective utilisation of the heat capacity of the liquid heat transfer fluid.

Analysis of the temperature fields shows that the temperature distribution along the length of the heat exchanger is non-uniform. In the inlet section of the apparatus, the air temperature remains close to the initial value ( $\approx 38\text{-}40$  °C), which is explained by insufficient contact time and a thermal boundary layer that has not yet fully developed. The most significant temperature drop is observed in the central zone of the heat exchanger, where the air temperature decreases to 25-30 °C. In the outlet section, the rate of temperature change slows down, which is associated with a reduction in the temperature head between the heat transfer fluids.

Water exhibits an inverse relationship: the most rapid rise in temperature occurs in the first half of the heat exchanger, after which the rate of heating decreases and the temperature gradually approaches that of the air. This indicates that the majority of the heat flux is transferred in the central zone of the unit, where the greatest temperature gradient is found.

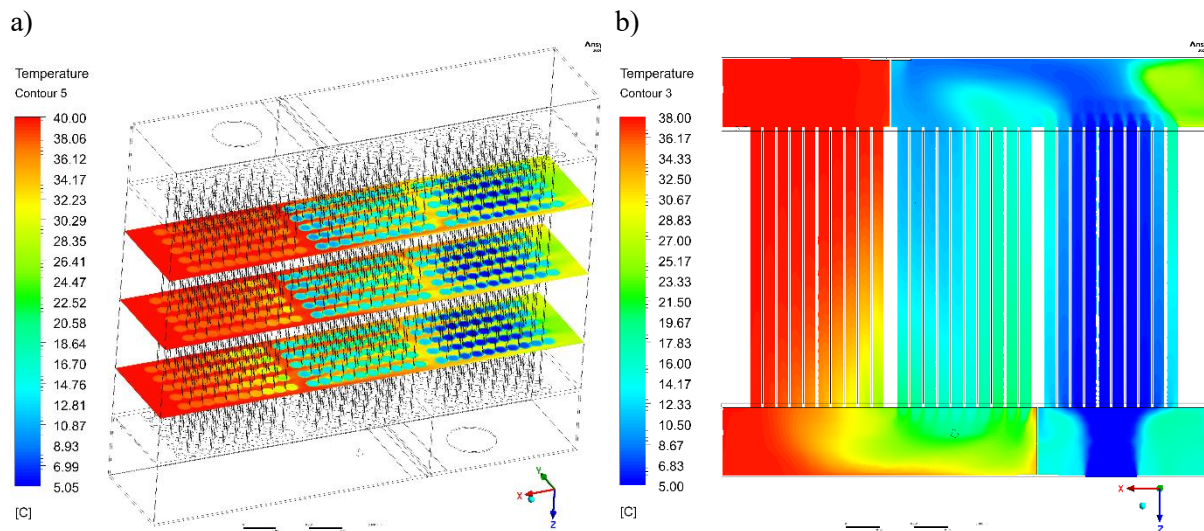


Fig. 5. Temperature distribution of air (a) along the  $yx$  line and water (b) along the central  $zx$  line in the heat transfer media of a compact tube bundle, °C

The temperature fields also demonstrate an uneven distribution across the cross-section. The temperature difference between individual channels reaches 5-10 °C, which is consistent with the previously established non-uniformity of the velocity field. In particular, in the high-velocity zones (inter-tube channels), more intense air cooling is observed, whilst in the near-surface regions of the casing and in the recirculation zones, the temperature remains higher. This indicates non-uniform utilisation of the heat exchange surface.

The measured heat flux values at the wall surface are approximately  $1500\text{-}1568\text{ W}\cdot\text{m}^{-2}$ , confirming the intense nature of the heat transfer. At the same time, the heat transfer coefficients on the water side ( $\approx 800\text{-}1200\text{ W}\cdot\text{m}^{-2}\cdot\text{K}^{-1}$ ) are 2-5 times higher than the corresponding values for the air ( $\approx 150\text{-}600\text{ W}\cdot\text{m}^{-2}\cdot\text{K}^{-1}$ ), indicating that thermal resistance is dominated by the gaseous heat transfer fluid.

Thus, the simulation results show that heat transfer efficiency is determined by a combination of high air flow turbulence. At the same time, the non-uniformity of the velocity field and the presence of zones with reduced velocities lead to the formation of temperature inhomogeneity, which limits the efficiency of individual sections of the heat exchanger and indicates the advisability of further optimisation of the channel geometry and flow distribution.

## Conclusions

1. A comprehensive analysis of the distributions of velocity, temperature and pressure shows that the efficiency of the heat exchanger under investigation is determined by a trade-off between heat transfer intensification and hydraulic losses. Local acceleration of the air to  $20\text{-}30\text{ m}\cdot\text{s}^{-1}$  in the inter-tube channels results in a temperature reduction of  $11.36\text{ }^{\circ}\text{C}$  (from  $40$  to  $28.64\text{ }^{\circ}\text{C}$ ) and the formation of a heat flux of  $1500\text{-}1568\text{ W}\cdot\text{m}^{-2}$ . At the same time, the water flow at a velocity of  $0.245\text{-}0.248\text{ m}\cdot\text{s}^{-1}$  ensures effective heat removal with a temperature rise of  $32.75\text{ }^{\circ}\text{C}$ .
2. It has been established that the intensification of heat transfer is accompanied by an increase in pressure drop of up to  $780\text{ Pa}$  for air and  $1200\text{ Pa}$  for water, as well as the formation of non-uniform velocity and temperature fields, where the temperature difference reaches  $5\text{-}10\text{ }^{\circ}\text{C}$ . This indicates that the heat transfer surface is not being fully utilised.
3. Thus, it is advisable to improve the efficiency of the heat exchanger by optimising the geometry of the inter-tube space and the inlet chambers, in particular by reducing recirculation zones and streamlining the flow, which will reduce hydraulic losses whilst maintaining high heat transfer intensity.

## Author contributions

Investigation, V.T. and L.K.; conceptualization, A.A., A.R.; methodology, Ye.B. and V.B.; software, O.S. All authors have read and agreed to the published version of the manuscript.

## References

- [1] Hojjat M. Nanofluids as coolant in a shell and tube heat exchanger: ANN modeling and multi-objective optimization. *Applied Mathematics and Computation*, 365, 2020, article number 124710. DOI: 10.1016/j.amc.2019.124710
- [2] Bichkar P., Dandgaval O., Dalvi P., Godase R., Dey T. Study of shell and tube heat exchanger with the effect of types of baffles. *Procedia Manufacturing*, 20, 2018, pp. 195-200. DOI: 10.1016/j.promfg.2018.02.028
- [3] Wang C., Cui Z., Yu H., Chen K., Wang J. Intelligent optimization design of shell and helically coiled tube heat exchanger based on genetic algorithm. *International Journal of Heat and Mass Transfer*, 159, 2020, article number 120140. DOI: 10.1016/j.ijheatmasstransfer.2020.120140
- [4] Tayyab M., Cheema T.A., Malik M.S., Muzaffar A., Sajid M.B., Park C.W. Investigation of thermal energy exchange potential of a gravitational water vortex. *Renewable Energy*, 162, 2020, pp. 1380-1398. DOI: 10.1016/j.renene.2020.08.097
- [5] Alam T., Kim M.H. A comprehensive review on single-phase heat transfer enhancement techniques in heat exchanger applications. *Renewable and Sustainable Energy Reviews*, 81, 2018, pp. 813-839. DOI: 10.1016/j.rser.2017.08.060
- [6] Feizabadi A., Khoshvaght-Aliabadi M., Rahimi A.B. Experimental evaluation of thermal performance and entropy generation inside a twisted U-tube equipped with twisted-tape inserts. *International Journal of Thermal Sciences*, 145, article number 106051. DOI: 10.1016/j.ijthermalsci.2019.106051
- [7] Talebi M., Lalgani F. Assessment of thermal behavior of variable step twist in the elliptical spiral. *International Journal of Thermal Sciences*, 170, 2019, article number 107126. DOI: 10.1016/j.ijthermalsci.2021.107126
- [8] Riaz M.T., Cheema T.A., Tayyab M., Khan A.U.A., Amber K.P., Sajid M.B., Park C.W. Investigation of free and forced vortex induced thermal energy exchange potential. *Sustainable Energy Technologies and Assessments*, 52, 2022, article number 102107. DOI: 10.1016/j.seta.2022.102107
- [9] Jamil M.A., Goraya T.S., Shahzad M.W., Zubair S.M. Exergoeconomic optimization of a shell-and-tube heat exchanger. *Energy Conversion and Management*, 226, 2020, article number 113462. DOI: 10.1016/j.enconman.2020.113462
- [10] Lim T.-W., Choi Y.-S. Thermal design and performance evaluation of a shell-and-tube heat exchanger using LNG cold energy in LNG fuelled ship. *Applied Thermal Engineering*, 171, 2020, article number 115120. DOI: 10.1016/j.applthermaleng.2020.115120

- [11] Gorobets V., Trokhaniak V., Bohdan Y., Antypov I. Numerical modeling of heat transfer and hydrodynamics in compact shifted arrangement small diameter tube bundles. *Journal of Applied and Computational Mechanics*, 7(1), 2021, pp. 292-301. DOI: 10.22055/JACM.2020.31007.1855
- [12] Trokhaniak V., Gorobets V., Shelimanova O., Balitsky A. Research of thermal and hydrodynamic flows of heat exchangers for different air-cooling systems in poultry houses. *Machinery & Energetics*, 14(1), 2023, pp. 68-78. DOI: 10.31548/machinery/1.2023.68